Mechanism of the UV band-edge photorefractivity enhancement in near-stoichiometric $LiNbO_3$*

XIN Fei-fei (辛非非)**
College of Physics and Materials Science, Tianjin Normal University, Tianjin 300387, China

(Received 7 March 2018; Revised 18 April 2018)

The UV photorefractive properties of near-stoichiometric $LiNbO_3$ single crystal are found to be significantly enhanced compared with the congruent one at 325 nm. The temperature dependence of the band edge of near-stoichiometric $LiNbO_3$ crystal is investigated. Significant thermal-induced spectral shift in band gap which obeys the Bose-Einstein expression is observed, and the fundamental band gap at zero absolute temperature is found to be much larger than the congruent one. New absorption bands near the UV band edge which are much stronger in the near-stoichiometric $LiNbO_3$ than those in the congruent $LiNbO_3$ crystal show up at temperatures lower than ~400 K. Note that the UV photorefractivity is enhanced in SLN, which has exactly the same tendency as the absorption strength.
Document code: A **Article ID:** 1673-1905(2018)05-0359-4
DOI https://doi.org/10.1007/s11801-018-8034-9

$LiNbO_3$ single crystals have been well studied as a material for holographic volume storage, optical image and signal processing, coherent optical amplification, and phase conjugation[1-7]. However, most crystals used for investigations and applications are congruent $LiNbO_3$ (CLN) with a large number of intrinsic defects induced by Li insufficiency, which limit their device performance in many cases. Compared with CLN, near-stoichiometric $LiNbO_3$ (SLN) is expected to reduce the concentration of these intrinsic defects and show some different optical properties from congruent one. In fact, people have found enhanced photorefractive properties in SLN in the visible region, which indicates that the change of the [Li]/[Nb] ratio plays an important role in the photorefractive process of $LiNbO_3$[8]. However, no one has ever made a clear explanation about the corresponding micromechanisms and in the UV region even less information has been reported. In this paper, we investigate the UV band edge photorefractivity, the thermal induced spectral properties of the fundamental band edge and the deep level defect structures of SLN.

Nominally pure $LiNbO_3$ crystals were grown using the Czochralski method. In order to obtain $LiNbO_3$ crystal with near stoichiometric composition, the vapor-transport-equilibration (VTE) technique was employed. The compositions of [Li]/([Nb]+[Li]) in SLN and CLN crystals are 49.9mol% and 48.5mol%, respectively. Both of the crystals were cut in the form of *Y*-oriented plates with the size of 15 mm×0.5 mm×12 mm ($x\times y\times z$). The photorefractive properties at 325 nm and UV band edge absorption spectra were detected for both CLN and SLN.

In order to get the UV band edge photorefractive properties of our samples, holographic gratings at 325 nm were written with $I_S=I_R=490$ mW/cm^2 and the crossing angle of the two beams is 32° in air. The grating wave vector is aligned along the c-axis of the sample. A third beam at 325 nm, expanded and incident at an off-Bragg angle when necessary, served as a uniform erasing beam. The buildup and decay dynamics of the gratings were monitored by a weak red probe beam at 633 nm incident at a Bragg-matched angle. The probe beam intensity was kept as low as 2 mW/cm^2 in order to avoid any detectable effect on the grating buildup and decay dynamics. During the measurement, we launched the two writing beams and the weak probe beam onto the crystal synchronously. After the diffracted beam intensity of the probe beam reached a saturated value, we turned off the two writing beams and launched the uniform UV erasing beam of 32.6 mW/cm^2 onto the crystal at the same time to study the erasing dynamics of the gratings.

The results of the above UV photorefractive properties of SLN and CLN are shown in Tab.1, where the values of the characteristic parameters can be found in Ref.[9] and textbooks such as Ref.[1]. One can see that the photorefractive properties of SLN are dramatically improved compared with CLN. An abrupt increase in diffraction efficiency from 1.42% to 3.95% and a significant increase in the holographic recording sensitivity (for ~2.5 times) appear between the samples CLN and SLN. The recording and optical erasing cycles with a temporal resolution of 5×10^{-4} s for CLN and SLN are shown in Fig.1. We can see that the gratings can be recorded and erased

* This work has been supported by the Doctoral Foundation of Tianjin Normal University (No.135202XB1607).
** E-mail: cindyfeifei@163.com

in a very short time interval in SLN compared with CLN, resulting in a sharp drop of the buildup response time from 2.57 s to 0.32 s, and a drastic increase in the specific photoconductivity σ_{ph}/I_e.

Tab.1 Measured UV photorefractive characteristics of CLN and SLN crystals at 325 nm

Characteristic	CLN	SLN
Diffraction coefficiency (%)	1.42	5.31
Response time (s)	2.57	0.32
Sensitivity (cm/J)	3.27	8.16
σ_{ph}/I_e (10^{-12} cm/ΩW)	1.79	27.05

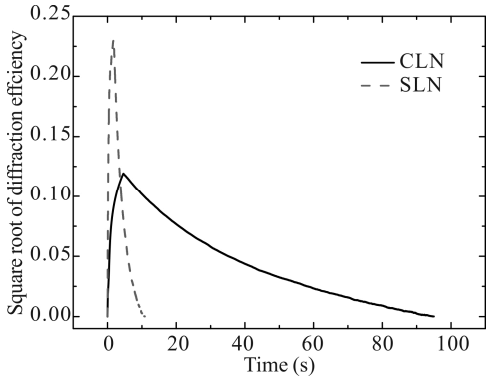

Fig.1 Holographic recording and optical erasing cycles in our samples at 325 nm

The UV band edge absorption spectra in the temperature range from 3.8 K to 973 K were measured for our samples. In order to achieve the cryogenic temperature, we placed the crystal in a cryogenic sample chamber, using the low temperature adhesive to fix it on a copper sample holder. First, a vacuum system was used to pump the low-temperature chamber into the vacuum with a pressure lower than 2×10^{-2} Pa. The vacuum pump system is composed of a mechanical pump and a molecular pump. The limiting pressure of the mechanical pump is 4×10^{-2} Pa, while the limiting pressure of the molecular pump is 6×10^{-7} Pa. During the experiment, the mechanical pump was turned on first. When the pressure of the sample chamber reached a level between 1 Pa and 10 Pa, we turned on the molecular pump to achieve a pressure lower than 2×10^{-2} Pa. The degree of vacuum was monitored by a digital composite vacuum gauge. When the pressure got lower than 2×10^{-2} Pa, the low-temperature refrigeration system Optistat AC-V by the Oxford Instruments was turned on. The low temperature system has a minimum temperature of 3 K with the temperature stability of ±0.15 K. The cryogenic sample chamber has four quartz optical windows to facilitate the detection of the passage of the light field. For higher temperatures from room temperature to 973 K, we used a temperature control heating system with the temperature stability of ±0.2 K, which has two quartz optical windows for optical detection.

The spectral dichroism of our samples was found to be negligible, therefore, the data presented in this paper is only for the extraordinary polarized light.

The absorption band edge was found to be red-shifted significantly with the increase of crystal temperature in both samples, therefore, the band energy gap E_g, defined as the photon energy at which α=70 cm^{-1}, decreases with the increase of temperature, as shown in Fig.2. The temperature dependence of E_g can be well described by the Bose-Einstein expression[10]

$$E_g(T) = E_{gBE}(0) - \frac{2a_B}{\exp(E_{pBE}/k_BT) - 1}, \quad (1)$$

where T is the absolute temperature, $E_{gBE}(0)$ is the fundamental band gap at T=0, α_B represents the strength of electron-phonon interaction, and E_{pBE} is the average energy of the Einstein oscillator corresponding to the most active phonons. Excellent fitting results for both CLN and SLN are also shown in Fig.2. The yielded values of $E_{gBE}(0)$, α_B and E_{pBE} are shown in Tab.2. Evidently, the shift of fundamental band gap $E_{gBE}(0)$ from CLN to SLN is as large as ~0.2 eV, which is larger than that at the room temperature as shown in Fig.2.

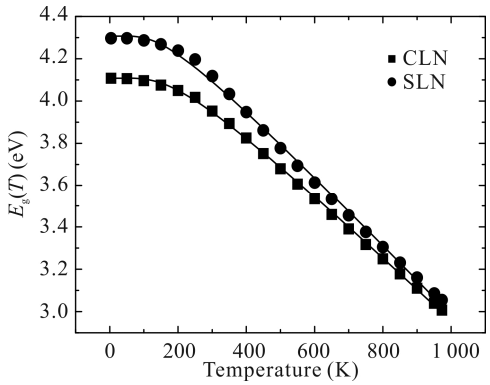

Fig.2 The measured temperature dependence of the fundamental band gap of CLN and SLN with corresponding fitting curves by the Bose-Einstein expression

The absorption edge tails of both samples at temperatures higher than 400 K are consistent with the widely observed Urbach rule[11]

$$\alpha = \alpha_0 \exp\left[\frac{\sigma}{k_BT^*}(\hbar\omega - \hbar\omega_0)\right], \quad (2)$$

where α_0, σ and ω_0 are constants, k_B is the Boltzman constant, $\hbar$ is the Planck constant, and T^* is the effective temperature determined by

$$T^* = \frac{\hbar\omega_p}{2k_B}\coth\left(\frac{\hbar\omega_p}{2k_BT}\right), \quad (3)$$

where ω_p is the phonon frequency at which the most active interaction occurs with electrons. Fig.3 shows the semi-logarithmic spectral plots of the absorption edge of SLN vs. photon energy $E=\hbar\omega$ from room temperature (300 K) to 900 K. However, as the temperature goes

down below ~400 K and the absorption edge shifts towards higher energy, an additional absorption band shows up at the bottom of the absorption edge tail. We found that although the profile of the absorption edge tail around this new band deviates from the Urbach rule, the remaining part of the absorption edge tail still obeys the Urbach rule, as demonstrated by the dashed line for 300 K in Fig.3. The energy of the most active phonons $E_{pU}=\hbar\omega_p$ was calculated for both samples by fitting the measured absorption edges using Eqs.(2) and (3), as shown in Tab.2. The energy E_{pU} of SLN shows a considerable reduction from CLN, which is quite similar to that of the Einstein oscillator E_{pBE}. In fact, the Urbach rule can also be well modeled by the Einstein oscillator[12]. In ionic crystals such as $LiNbO_3$, the slopes of the spectral Urbach rule have been correlated with the strength of the polaron coupling[13].

Tab.2 The fitting characteristics for the UV absorption band tails of CLN and SLN crystals by Bose-Einstein expression and Urbach law

Characteristic	CLN	SLN
$E_{gBE}(0)$ (eV)	4.108	4.307
α_B (eV)	0.422	0.378
E_{pBE} (cm^{-1})	381.8	313.7
E_{pU} (cm^{-1})	378.6	321.4

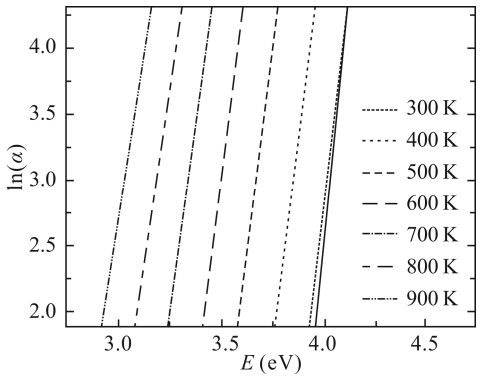

Fig.3 Spectral profiles of ln(*α*) for SLN at different temperatures

As the temperature goes down below 400 K and the absorption edge of the crystal is blue-shifted gradually, a new absorption band at the bottom of the Urbach tail shows up in both samples. Typical absorption spectra at a cryogenic temperature of 3.8 K for both samples are shown in Fig.4(a). It is the appearance of this new absorption band that deforms the Urbach tail at this spectral region, as we have mentioned above. In order to show the true spectral structure of this absorption band, we subtract the Urbach tail from the measured spectra and get[14]

$$\Delta\alpha=\alpha-\alpha_0\exp[\frac{\sigma}{k_BT^*}(\hbar\omega-\hbar\omega_0)], \quad (4)$$

where α_0, σ, ω_0 and T^* can be extracted by fitting the remaining spectrum without deformation to the Urbach rule. The calculated spectral profiles of $\Delta\alpha$ measured at 3.8 K for CLN and SLN are shown in Fig.4(b). We attribute the observed absorption band $\Delta\alpha$ at the bottom of the Urbach tail to the formation of O^- polarons near the negatively charged defect centers in crystal. Because of the Li deficiency, there will be a lot of lithium vacancy V_{Li} centers and the O^- polaron can be formed when a hole is trapped at an oxygen ion near a lithium vacancy (O^--V_{Li}). However, it is quite easy for those O^- polarons to recombine with $Nb_{Li}^{5+/4+}$ directly, so the existence of Nb_{Li}^{5+} will shorten the lifetime of small polarons (O^--V_{Li})[15,16]. As proposed by Berben et al, the depopulation rate of small polarons shows a stretched exponential behavior and the lifetime of an individual polaron depends on the distance to the nearest trap[17]. More stoichiometric composition of SLN reduces the concentrations of both Nb_{Li}^{5+} and V_{Li}, so the averaged distance between the polarons becomes larger. Therefore, we find that the peak of the absorption band $\Delta\alpha_p$ grows significantly with the increase of [Li]/[Nb], as shown in Fig.4(a) and (b). The peak of the absorption band $\Delta\alpha$ of SLN is higher than that of the CLN. Note that the UV photorefractivity is enhanced in SLN, which has exactly the same tendency as the absorption strength α shown in Fig.4. In addition, the absorption band $\Delta\alpha$ of CLN and SLN can be fitted by a Gaussian peak at 3.83 eV and 3.93 eV, respectively.

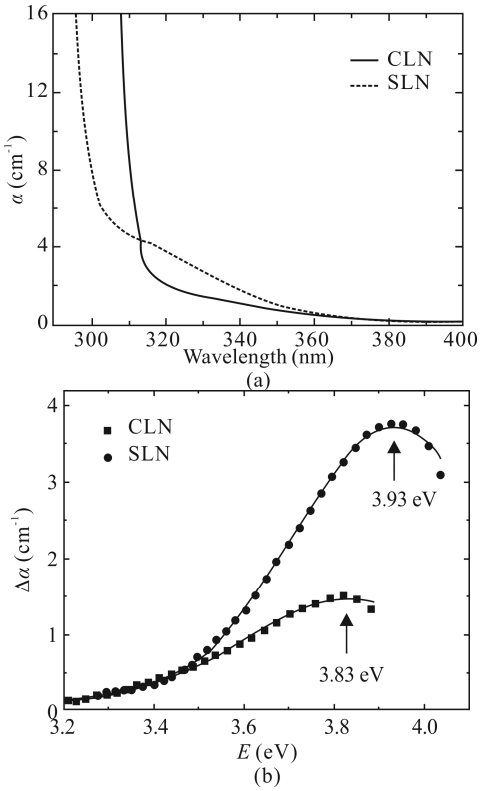

Fig.4 (a) Absorption spectra of CLN and SLN crystals at 3.8 K; (b) Spectral profiles of Δ*α* measured at 3.8 K for CLN and SLN with their theoretical Gaussian fitting profiles peaked at 3.83 eV and 3.93 eV, respectively

In summary, the UV band edge photorefractivity, the UV band edge spectra and the UV photo-sensitive defect centers of $LiNbO_3$ with different compositions have been studied. The absorption band edge is the type of the phonon-induced Urbach tail, the temperature dependence of the energy gap obeys the Bose-Einstein expression, and the fundamental band gap has been found to increase with the increase of Li concentration. A new absorption band at the bottom of the Urbach tail appears in both samples at low temperatures, and it is attributed to the O^- polarons trapped near the V_{Li} centers, which act as important photo-sensitive centers in the UV photorefraction of $LiNbO_3$ with different compositions.

References

[1] T. Volk and M. Wöhlecke, Lithium Niobate: Defects, Photorefraction and Ferroelectric Switching, Springer-Verlag, Berlin, 2008.

[2] B. Tian, H. Chen, D. Choge, Y. Xu, G. Li and W. Liang, Optoelectron. Lett. 1**3**, 206 (2017).

[3] W. Wu, J. Ma, H. Pan, E. Wu, H. Chen, K. Dismas and W. Liang , Optoelectron. Lett. **13**, 156 (2017).

[4] S. Pal, B. Das and S. Wolfgang, Appl. Phys. B **120**, 737 (2015).

[5] D. Zheng, Y. Kong, S. Liu, M. Chen, S. Chen, L. Zhang, R. Rupp and J. Xu, Sci. Rep. **6**, 20308 (2016).

[6] D. Zheng, Y. Kong, S. Liu, J. Yao, L. Zhang, S. Chen and J. Xu, AIP Adv. **1**, 031501 (2015).

[7] J. Wang, B. Zhu, Z. Hao, F. Bo, X. Wang, F. Gao, Y. Li, G. Zhang and J. Xu, Opt. Express **24**, 21869 (2016).

[8] X. Chen, B. Li, J. Xu, D. Zhu, S. Pan and Zh. Wu, J. Appl. Phys. **90**, 1516 (2001).

[9] F. Xin, G. Zhang, F. Bo, H. Sun, Y. Kong, J. Xu, T. Volk and N. Rubinina, J. Appl. Phys. **107**, 033113 (2010).

[10] L. Viña, S. Logothetidis and M. Cardona, Phys. Rev. B **30**, 1979 (1984).

[11] J. Castillo-Torres, Opt. Commun. **290**, 107 (2013).

[12] G. D. Cody, T. Tiedje, B. Abeles, B. Brooks and Y. Goldstein, Phys. Rev. Lett. **47**, 1480 (1981).

[13] J. D. Dow and D. Redfield, Phys. Rev. B **5**, 594 (1972).

[14] F. Xin, Z. Zhai, X. Wang, Y. Kong, J. Xu and G. Zhang, Phys. Rev. B **86**, 165132 (2012).

[15] P. Herth, T. Granzow, D. Schaniel, Th. Woike, M. Imlau and E. Krätzig, Phys. Rev. Lett. **95**, 067404 (2005).

[16] C. Merschjann, B. Schoke and M. Imlau, Phys. Rev. B **76**, 085114 (2007).

[17] D. Berben, K. Buse, S. Wevering, P. Herth, M. Imlau and Th. Woike, J. Appl. Phys. **87**, 1034 (2000).